Life Sciences 230 (2019) 55–67

Contents lists available at ScienceDirect

Life Sciences

journal homepage: www.elsevier.com/locate/lifescie

Activation of cannabinoid type 2 receptor protects skeletal muscle from ischemia-reperfusion injury partly *via* Nrf2 signaling

Mengzhou Zhang[a], Miao Zhang[a,b,c], Linlin Wang[a,b,c], Tianshui Yu[b], Shukun Jiang[a,b,c], Penghao Jiang[a], Yingfu Sun[a], Jingbo Pi[d], Rui Zhao[a,b,c,*], Dawei Guan[a,b,c,*]

[a] Department of Forensic Pathology, China Medical University School of Forensic Medicine, Shenyang 110122, China
[b] Remote Forensic Consultation Center, Collaborative Innovation Center of Judicial Civilization, China University of Political Science and Law, Beijing 100192, China
[c] Collaborative Laboratory of Intelligentized Forensic Science (CLIFS), Shenyang 110032, China
[d] Program of Environmental Toxicology, China Medical University School of Public Health, Shenyang 110122, China

ARTICLE INFO

Keywords:
Cannabinoid type 2 receptor
Ischemia-reperfusion injury (IRI)
Oxidative stress
NF-E2-related factor (Nrf2)
AM1241
Myogenesis

ABSTRACT

Aims: Cannabinoid type 2 (CB_2) receptor activation has been shown to attenuate IRI in various organs. NF-E2-related factor (Nrf2) is an anti-oxidative factor that plays multiple roles in regulating cellular redox homeostasis and modulating cell proliferation and differentiation. The protective effects of CB_2 receptor activation on skeletal muscle IRI and the underlying mechanism that involves Nrf2 signaling remain unknown.

Main methods: We evaluated the *in vivo* effect of CB_2 receptor activation by the CB_2 receptor agonist AM1241 on IR-induced skeletal muscle damage and early myogenesis. We also assessed the effects of CB_2 receptor activation on C2C12 myoblasts differentiation and H_2O_2-induced C2C12 myoblasts damage *in vitro*, with a focus on the mechanism of Nrf2 signaling.

Key findings: Our results showed that CB_2 receptor activation reduced IR-induced histopathological lesions, edema, and oxidative stress 1 day post-injury and accelerated early myogenesis 4 days post-injury in mice. *Nrf2* knockout mice that were treated with AM1241 exhibited deteriorative skeletal muscle oxidative damage and myogenesis. *In vitro*, pretreatment with AM1241 significantly increased the expression of Nrf2 and its nuclear translocation, attenuated the decrease in H_2O_2-induced C2C12 cell viability, and decreased reactive oxygen species generation and apoptosis. CB_2 receptor activation also significantly enhanced C2C12 myoblasts differentiation, which was impaired by silencing Nrf2.

Significance: Overall, CB_2 receptor activation protected skeletal muscle against IRI by ameliorating oxidative damage and promoting early skeletal muscle myogenesis, which was partly *via* Nrf2 signaling.

1. Introduction

Skeletal muscle ischemia-reperfusion injury (IRI) is a common and severe clinical disease with high morbidity and mortality, usually secondary to vascular injury, crush syndrome, compartment syndrome, reconstruction surgery, or the use of surgical tourniquets [1,2]. Skeletal muscles have high metabolic activity and are sensitive to IRI [3]. The mechanisms of IRI are complex. Reactive oxygen species (ROS) are considered to be a main factor in local and systemic damage caused by IRI [1]. As blood reperfuses, abundant ROS are generated, leading to skeletal muscle oxidative stress that consequently causes the necrosis of skeletal muscle myocytes [4]. Skeletal muscles have a robust regeneration capacity. Satellite cells (SCs) are essential for muscle regeneration and initiate and regulate the repair process after injury that basically recapitulates myogenesis [5]. SCs proliferation and differentiation are regulated by the myogenic regulatory factor (MRF) family, consisting of MyoD and myogenin. MyoD induces SCs proliferation, and myogenin induces cell-cycle arrest and differentiation. Skeletal muscle regeneration is believed to be tightly controlled by redox balance [6]. Excessive oxidative stress can cause skeletal muscle damage and impair subsequent regeneration [7–9].

The cannabinoid type 2 (CB_2) receptor is a seven-transmembrane, G protein-coupled receptor that is widely expressed in various tissues, including heart, liver, brain, and skeletal muscle [10,11]. CB_2 receptor has been shown to have anti-oxidative and anti-inflammatory effects and has emerged as a promising therapeutic target for various

* Corresponding authors at: Department of Forensic Pathology, China Medical University School of Forensic Medicine, No.77, Puhe Road, Shenyang North New Area, Shenyang 110122, Liaoning Province, China.
E-mail addresses: rzhao@cmu.edu.cn (R. Zhao), dwguan@cmu.edu.cn (D. Guan).

https://doi.org/10.1016/j.lfs.2019.05.056
Received 21 March 2019; Received in revised form 18 May 2019; Accepted 21 May 2019
Available online 22 May 2019

disorders, including inflammation and tissue injury [12,13]. Our previous studies found that CB_2 receptor activation attenuated the inflammatory response and improved muscle repair after skeletal muscle contusion in rats [14,15]. CB_2 receptor protein levels significantly increased during murine C_2C_{12} myoblasts and primary human skeletal muscle cell (hSkMC) differentiation [16]. Therefore, we speculated that CB_2 receptor activation might have beneficial effects on skeletal muscle IRI.

NF-E2-related factor (Nrf2) plays a pivotal role in the cellular defense against oxidative stress [17,18]. Under physiological conditions, Nrf2 is retained in the cytoplasm and degraded by its inhibitor Keap1. Oxidative stress stimuli disrupt the Nrf2/Keap1 complex. Nrf2 is activated and translocated into the nucleus, eventually resulting in an increase in the expression of antioxidant genes, such as heme oxygenase-1 (HO-1), to resist injury by binding to antioxidant response elements in the promoter regions of target genes [18]. Recently evidences suggest that Nrf2 has various novel functions, particularly in cell proliferation and differentiation [19]. Nrf2 deletion was shown to exacerbate cell apoptosis and subsequently impair skeletal muscle regeneration following injury in mice [5,8,9], suggesting that modulation of Nrf2 might be a potential strategy to treat skeletal muscle injury. Moreover, *in vivo* [20,21] and *in vitro* [22,23] evidences indicate that CB_2 receptor activation can functionally enhance Nrf2.

In the present study, we used *in vivo* and *in vitro* models to test the hypothesis that CB_2 receptor activation exerts beneficial effects on skeletal muscle IRI. The results showed that CB_2 receptor activation by the CB_2 receptor agonist AM1241 attenuated IR-induced skeletal muscle oxidative damage and promoted early myogenesis partially through Nrf2 signaling.

2. Materials and methods

2.1. Animal studies

Young, 8- to 12-week-old male C57BL/6 mice (wildtype; Charles River Laboratories) and *Nrf2* gene knockout mice on a C57BL/6 background (originally generated by Dr. Masayuki Yamamoto) were used. All of the mice were specific-pathogen-free grade and kept in our animal facility under pathogen-free conditions on a 12 h/12 h light/dark cycle. *Nrf2* knockout mice were confirmed according to a previous report [24] (Supplementary Fig. S1A, B). The wildtype mice were assigned to four groups: mice that were subjected to sham surgery (sham group), mice that were subjected to IR (IR group), mice that were subjected to IR and received vehicle (vehicle group), mice that were subjected to IR and received AM1241 (AM1241 group). *Nrf2* knockout mice were subjected to IR and received AM1241. Sterile injury was induced by a tourniquet for 2.5 h as described previously [25]. The mice were anesthetized with sodium pentobarbital (30 mg/kg, intraperitoneally) before model induction and skeletal muscle tissue sample (including gastrocnemius and tibialis anterior) collection. The mice were sacrificed 1 and 4 days after injury. The animal protocols conformed to the Guide for the Care and Use of Laboratory Animals (National Institutes of Health, publication no. 86-23, revised 1985) and were approved by the ethics committee of China Medical University.

2.2. Histological and immunohistochemical procedures

Hindlimb skeletal muscle tissue samples were collected, fixed in 4% paraformaldehyde, embedded in paraffin wax, cut into 5-μm sections, and stained with H&E for general staining. The sections or C2C12 myoblasts were also immunostained with antibodies against Nrf2, MPO, and the CB_2 receptor (see Supplementary material, Table S1). Immunofluorescence for Nrf2, MyoD, myogenin, MPO, MHC, dystrophin, and CB_2 receptor was detected using secondary antibodies conjugated with Alexa Fluor 594 or Alexa Fluor 488 (see Supplementary material, Table S1). Nuclei were counterstained with hematoxylin for immunohistochemistry or stained with DAPI for immunofluorescence. Control sections were similarly treated, with the exception of the primary antibody. All of the sections were visualized under a Leica DMi8 fluorescence microscope (Leica, Wetzlar, Germany). The destruction score was calculated according to a previous study by three independent pathologists [26]. Briefly, Sections stained with H&E were microphotographed from five random fields under ×400 magnification. Blinded observers were responsible for scoring morphological impairment based on muscle fiber disorganization and degeneration, and infiltration of neutrophils. Each criterion was graded between 0 points for normal findings to 3 points for very distinctive findings.

2.3. Wet weight/dry weight ratio of skeletal muscle

The muscle samples were weighed (wet weight) immediately after being harvested from the right hindlimb. The muscles were dehydrated at 60 °C for 72 h and then weighed again (dry weight). Tissue edema was characterized by the W/D ratio: W/D ratio = (wet weight / dry weight) × 100%.

2.4. Biochemical analyses of malondialdehyde and superoxide dismutase activity

Malondialdehyde levels and SOD activity in skeletal muscle tissues were measured using commercially available assay kits (A003-1-2 and A001-3-2, Nanjing Jiancheng Bioengineering Institute, Nanjing, China) according to the manufacturer's protocols. Briefly, at 1 day after skeletal muscle IRI, mice were perfused with cold PBS only, and the muscle samples were collected. Then samples were homogenized in nine volumes (grams per liter) of ice-cold saline and centrifuged at 12,000*g* for 15 min at 4 °C. The supernatant was used to measure the MDA content and the SOD activity using a spectrophotometer by comparing the optical density at 532 nm or 450 nm to standard curves. The total protein concentrations were quantified with a BCA assay kit (P0011, Beyotime, Shanghai, China). The content of MDA was expressed as nmol/g protein and SOD activity as U/mg protein.

2.5. Cell culture

The mouse skeletal muscle cell line C2C12 myoblasts (CRL-1772™, ATCC, Manassas, VA, USA), was cultured in high-glucose Dulbecco's modified Eagle's medium (DMEM) supplemented with 10% fetal bovine serum (FBS) and 100 μg/ml penicillin/streptomycin antibiotics at 37 °C with 5% CO_2. To induce myogenic differentiation, the proliferation medium (PM) was switched to differential medium (DM; DMEM with 2% horse serum (HS)) after C2C12 myoblasts growth had reached nearly 90% confluence. DMEM, FBS and HS were purchased from Life Technologies (Shanghai, China).

2.6. Cell viability assay

C2C12 myoblasts were seeded in 96-well culture plates (8×10^3 cells per well) and incubated overnight. The myoblasts were treated with 1, 2, 5 and 10 μM AM1241 (S1544, Selleck Chemicals, Houston, Texas, USA) in the presence or absence of 1 mM H_2O_2 (216763, Sigma, Burlington, Massachusetts, USA) for 12 h. The effect of AM1241 on the inhibition of cell growth was measured as the percentage of cell viability, which was assessed by the Cell Counting Kit-8 (CK04, Dojindo, Kumamoto, Japan) according to the manufacturer's protocol. Cell Counting Kit-8 solution (20 μl) was added to the medium, and myoblasts were incubated for 1 h in a humidified 5% CO_2 atmosphere. The amount of orange formazan staining was calculated by measuring absorbance at 450 nm using a microplate reader (Molecular Devices, Sunnyvale, CA, USA).

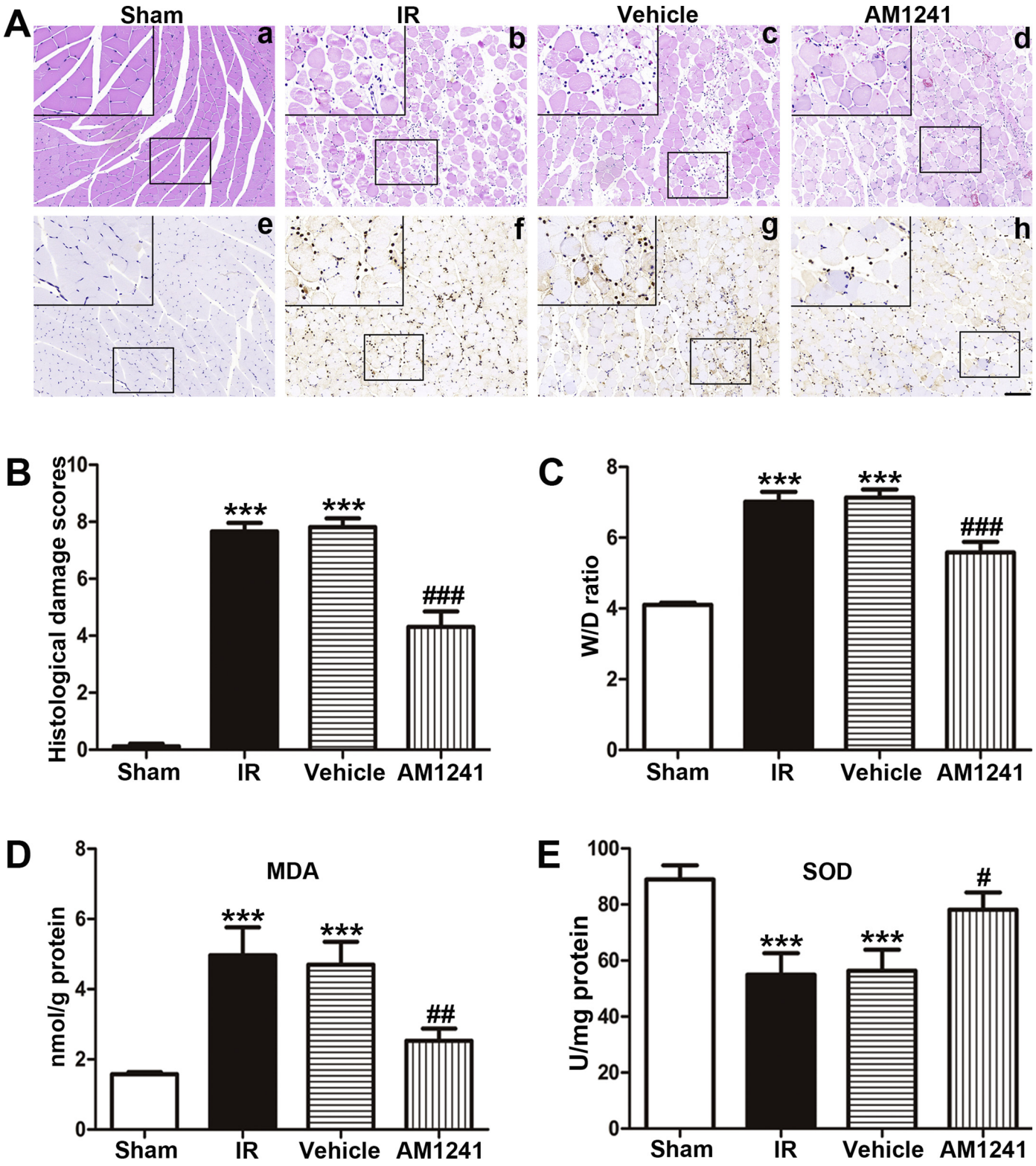

Fig. 1. Protective effects of CB_2 receptor activation against oxidative damage in skeletal muscle in mice subjected to IRI. (A) Representative images of skeletal muscle 1 day after IRI showing staining with H&E (upper panel) and immunohistochemical staining with MPO (lower panel) in the sham group (a, e), IR group (b, f), vehicle group (c, g), and AM1241 group (d, h). Scale bar = 100 μm. (B) Quantification of histological damage scores in the different groups. (C) W/D ratios for IR-induced tissue edema in skeletal muscle in the different groups. (D, E) Malondialdehyde levels and SOD activity in muscle tissue in the different groups. The data are expressed as mean ± SD. $^{***}p < 0.001$, compared with sham group; $^{\#}p < 0.05$, $^{\#\#}p < 0.01$, $^{\#\#\#}p < 0.001$, compared with vehicle group ($n = 6$).

2.7. Reactive oxygen species measurement

C2C12 myoblasts were plated in six-well plates at a density of 1×10^5 cells per well and treated with or without 5 μM or 10 μM AM1241 for 12 h and then incubated with or without 1 mM H_2O_2 for 6 h. The myoblasts were incubated with 10 μM 2′,7′-

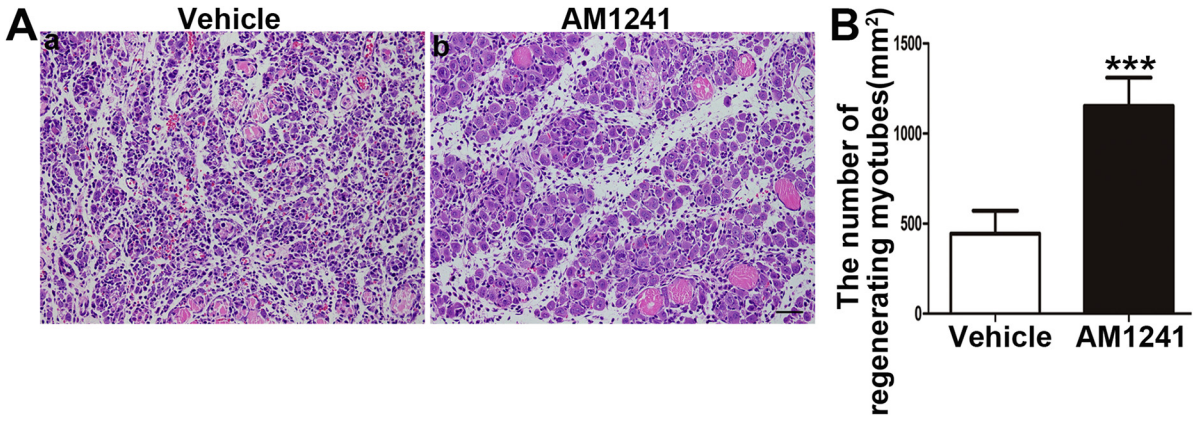

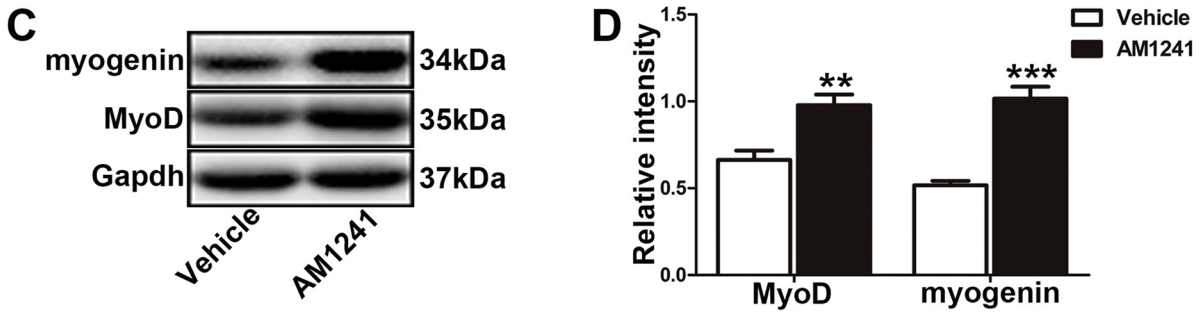

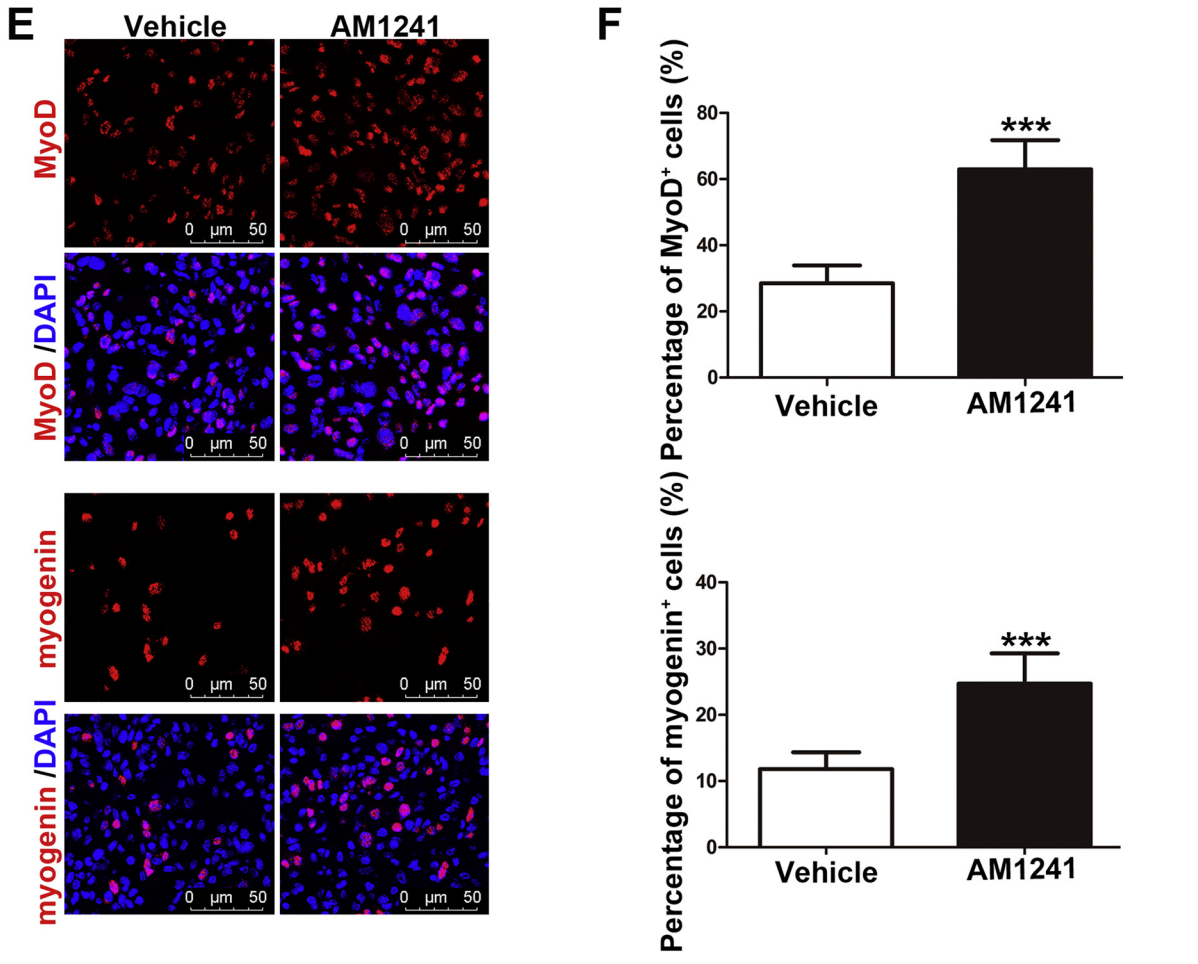

(caption on next page)

Fig. 2. CB_2 receptor activation promoted early myogenesis in mice subjected to IRI. (A) Representative images of skeletal muscle 4 days after IRI showing H&E staining in the vehicle group (a) and AM1241 group (b). Scale bar = 100 μm. (B) Quantification of the number of regenerating myotubes in the different groups. (C) Protein expression of MyoD and myogenin 4 days after skeletal muscle IRI. (D) Quantification of MyoD and myogenin protein levels. (E) Immunofluorescent staining of MyoD and myogenin (red), with nuclei stained with DAPI (blue). Scale bar = 50 μm. (F) Ratios of $MyoD^+$/$myogenin^+$ nuclei to the total number of skeletal muscle nuclei. The data are expressed as mean ± SD. $^{**}p < 0.01$, $^{***}p < 0.001$, compared with vehicle group ($n = 6$). (For interpretation of the references to colour in this figure legend, the reader is referred to the web version of this article.)

dichlorofluorescein diacetate (DCFH-DA, S0033, Beyotime, Shanghai, China) for the last 1 h at 37 °C in the dark. The myoblasts were immediately analyzed using a FACSCanto II device (BD Biosciences, San Jose, CA, USA). A total of 10,000 myoblasts per sample were acquired and analyzed using FlowJo X Software.

2.8. Annexin V-propidium iodide assay

Apoptosis was assessed using an Annexin V-FITC Apoptosis Analysis Kit (556547, BD Biosciences, San Jose, CA, USA). C2C12 myoblasts were seeded in a six-well plate at a density of 1×10^5 cells per well and treated with or without 5 μM or 10 μM AM1241 for 12 h. The cells were then treated in the presence or absence of 1 mM H_2O_2 for 6 h. The cell pellets were resuspended in 100 μl of buffer with 5 μl of annexin V-FITC and 5 μl of propidium iodide for 15 min at room temperature in the dark. A total of 500 μl of buffer was added, and the myoblasts were immediately analyzed using a FACSCanto II device (BD Biosciences, San Jose, CA, USA). A total of 10,000 myoblasts per sample were acquired, and the percentage of cell death was analyzed using FlowJo X Software.

2.9. Western blot analysis

Cold RIPA lysis buffer (pH 7.4), and Nuclear and Cytoplasmic Protein Extraction Kit (P0013B and P0028, Beyotime, Shanghai, China) that contained 2% phosphatase inhibitor cocktail (P1092, Beyotime, Shanghai, China) and 1 mM phenylmethylsulfonyl fluoride (ST506, Beyotime, Shanghai, China) were used for the whole-cell or nuclear and cytoplasmic lysates. Protein concentrations were detected using the BCA method (P0011, Beyotime, Shanghai, China) according to the manufacturer's instructions. Equal amounts of protein were separated by 10% sodium dodecyl sulfate-polyacrylamide gel electrophoresis, transferred to polyvinylidene fluoride membranes, and detected with target primary antibodies (see Supplementary material, Table S1) at 4 °C overnight. The membranes were incubated for 2 h at room temperature with the appropriate secondary horseradish peroxidase-conjugated antibody (see Supplementary material, Table S1) and visualized using an ECL detection kit (Millipore, Billerica, MA, USA). The densities of specific bands were quantified using ImageJ software.

2.10. Lentiviral-based shRNA transduction

MISSION shRNA lentivirus vectors were obtained from Sigma, and lentiviral particles were prepared according to the manufacturer's protocol. The lentiviral transduction of C2C12 myoblasts with particles for shRNAs that targeted Nrf2 (SHVRSNM_010902) or scrambled (Scr) non-target negative control (SHC002V) was performed as described previously [27]. Briefly, 24 h before transduction, C2C12 myoblasts were plated in 6-well plates at 40–50% confluence in PM. At following day, hexadimethrine bromide (H9268, Sigma, Burlington, Massachusetts, USA), a transduction enhancer, was added at a concentration of 8 μg/ml, and viral particles were added at a concentration of 2×10^5 transducing units/ml. After overnight incubation, medium containing viral particles was removed and replaced with fresh medium containing 1 μg/ml puromycin to select cells with stable silencing (*i.e.*, knockdown) and obtain a cell phenotype of *Nrf2* knockout.

2.11. Gene expression assessment

Total RNA extraction ($n = 6$/group) and reverse-transcription quantitative polymerase chain reaction (RT-qPCR) were performed as detailed elsewhere. Primer sequences are listed in Supplementary Table S2. To ensure that equal amounts of cDNA were added to the PCR reactions, the housekeeping gene *Gapdh* or *Actb* was amplified. The data were analyzed using the $^{\Delta\Delta}$CT comparative method. All of the PCR reactions were performed in triplicate.

2.12. Statistical analysis

The data are expressed as the mean ± standard deviation of at least three independent experiments. One-way analysis of variance followed by Tukey's Honestly Significant Difference *post hoc* test or Student's two-tailed unpaired *t*-test was used to measure differences between mean values of the different treated groups. Values of $p < 0.05$ were considered statistically significant. The data were analyzed using Prism 6.0 software (GraphPad, San Diego, CA, USA).

3. Results

3.1. CB_2 receptor activation ameliorated skeletal muscle oxidative damage in mice that were subjected to IRI

We first evaluated CB_2 receptor-expressing cells 1 day after IRI in mice. Double immunofluorescent staining showed that almost all of the infiltrated neutrophils were CB_2 receptor-positive (Supplementary Fig. S1C). We then evaluated the degree of skeletal muscle damage 1 day after IRI. The assessment of muscular tissue injury was based on morphological changes in hematoxylin and eosin (H&E) staining. Cytoplasmic fragmentation, blurred cell borders, the loss of nuclei, and neutrophil infiltration were observed in muscular tissue in the IR and vehicle groups (Fig. 1Ab, c, f, g) but not in the sham group (Fig. 1Aa, e). Histological damage scores significantly increased in the IR and vehicle groups compared with the sham group, but no significant difference was found between the IR and vehicle groups (Fig. 1B). The treatment of IR mice with AM1241 significantly reduced muscle injury, reflected by less sarcoplasm dissolution, a decrease in the loss of nuclei, and a decrease in neutrophil infiltration compared with the vehicle group (Fig. 1B). The wet weight/dry weight (W/D) ratio of skeletal muscle in the IR and vehicle groups significantly increased compared with the sham group. The W/D ratio in the AM1241 group significantly decreased compared with the vehicle group (Fig. 1C). The assessment of oxidative stress status showed that malondialdehyde (MDA) levels significantly increased and superoxide dismutase (SOD) activity significantly decreased in the IR and vehicle groups compared with the sham group (Fig. 1D, E). Treatment with AM1241 significantly reduced tissue MDA levels and increased tissue SOD activity compared with the vehicle group (Fig. 1D, E). Altogether, these results indicate that CB_2 receptor activation ameliorated IR-induced skeletal muscle damage and oxidative stress.

3.2. CB_2 receptor activation promoted early myogenesis in mice that were subjected to IRI

CB_2 receptor immunoreactivity was detected in regenerating myotubes (Supplementary Fig. S1D). H&E and immunofluorescent staining

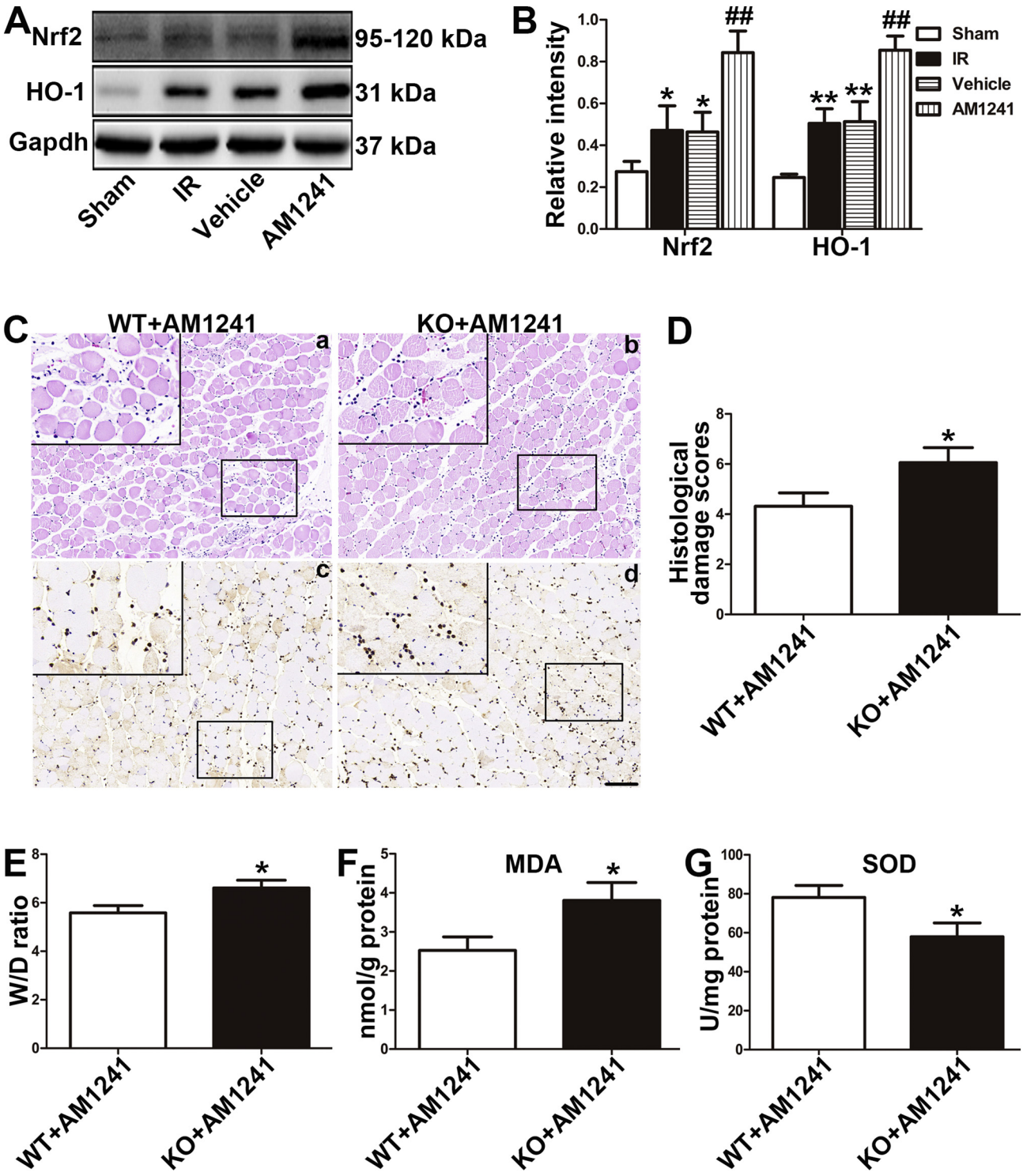

Fig. 3. Involvement of Nrf2 signaling in the effect of CB_2 receptor activation against oxidative damage in mice subjected to skeletal muscle IRI. (A) Protein expression of Nrf2 and HO-1 1 day after skeletal muscle IRI. (B) Quantification of Nrf2 and HO-1 protein levels. The data are expressed as mean ± SD. $^{*}p < 0.05$, $^{**}p < 0.01$, compared with sham group; $^{\#\#}p < 0.01$, compared with vehicle group ($n = 6$). (C) Representative photomicrographs of skeletal muscle tissue 1 day after IRI showing staining with H&E (upper panel) and immunohistochemical staining with MPO (lower panel) in the WT + AM1241 group (a, c) and *Nrf2* knockout + AM1241 group (b, d). Scale bar = 100 μm. (D) Quantification of histological damage scores. (E) W/D ratios for IR-induced tissue edema in skeletal muscle. (F, G) Malondialdehyde levels and SOD activity in muscle tissue. The data are expressed as mean ± SD. $^{*}p < 0.05$, compared with WT + AM1241 group ($n = 6$).

showed that AM1241-induced CB_2 receptor activation significantly increased the number of regenerating myotubes compared with the vehicle group 4 days post-injury (Fig. 2A, B and Supplementary Fig. S2A, B). MyoD and myogenin protein expression significantly increased in the AM1241 group 4 days after reperfusion compared with the vehicle group (Fig. 2C, D). To further confirm these findings, immunofluorescent staining was performed (Fig. 2E, F). The AM1241 group exhibited significant increases in MyoD- and myogenin-positive nuclei compared with the vehicle group (62.98% ± 8.12% *vs.* 28.48% ± 5.01% and 24.71% ± 4.29% *vs.* 11.83% ± 2.26%,

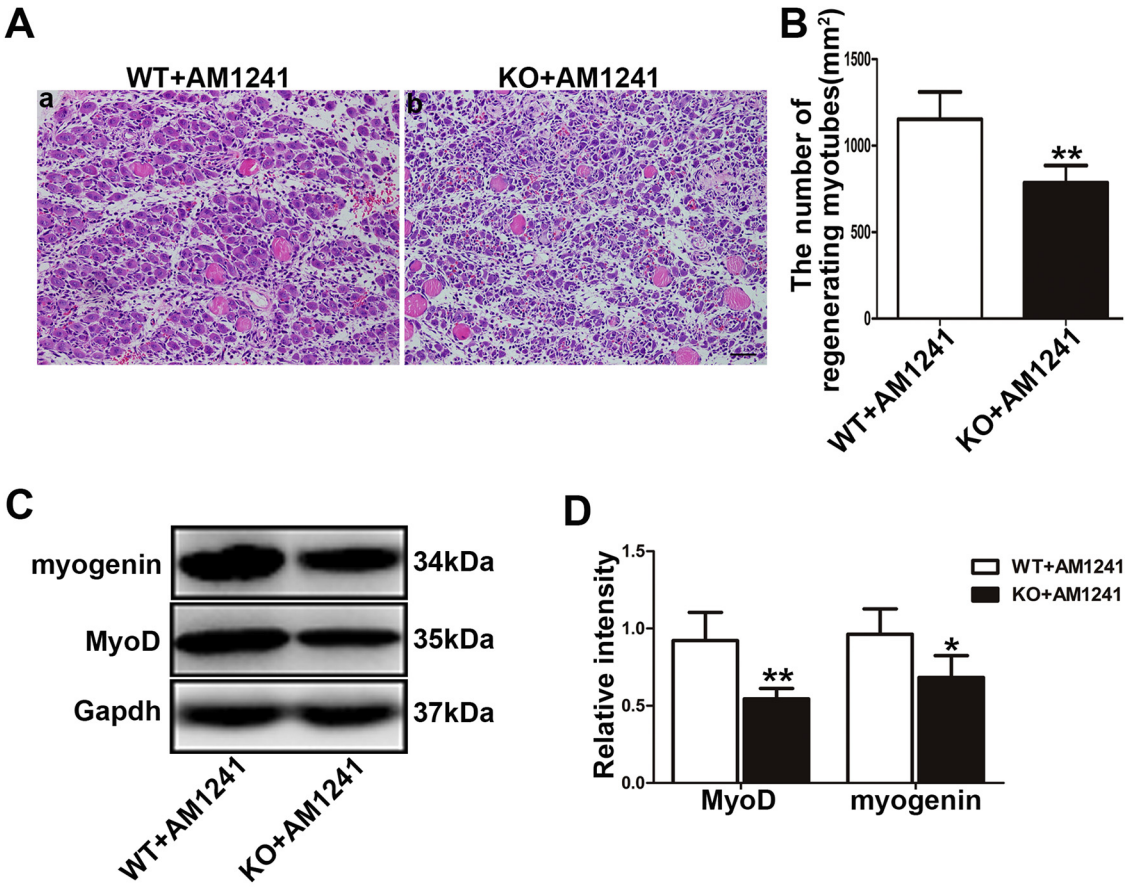

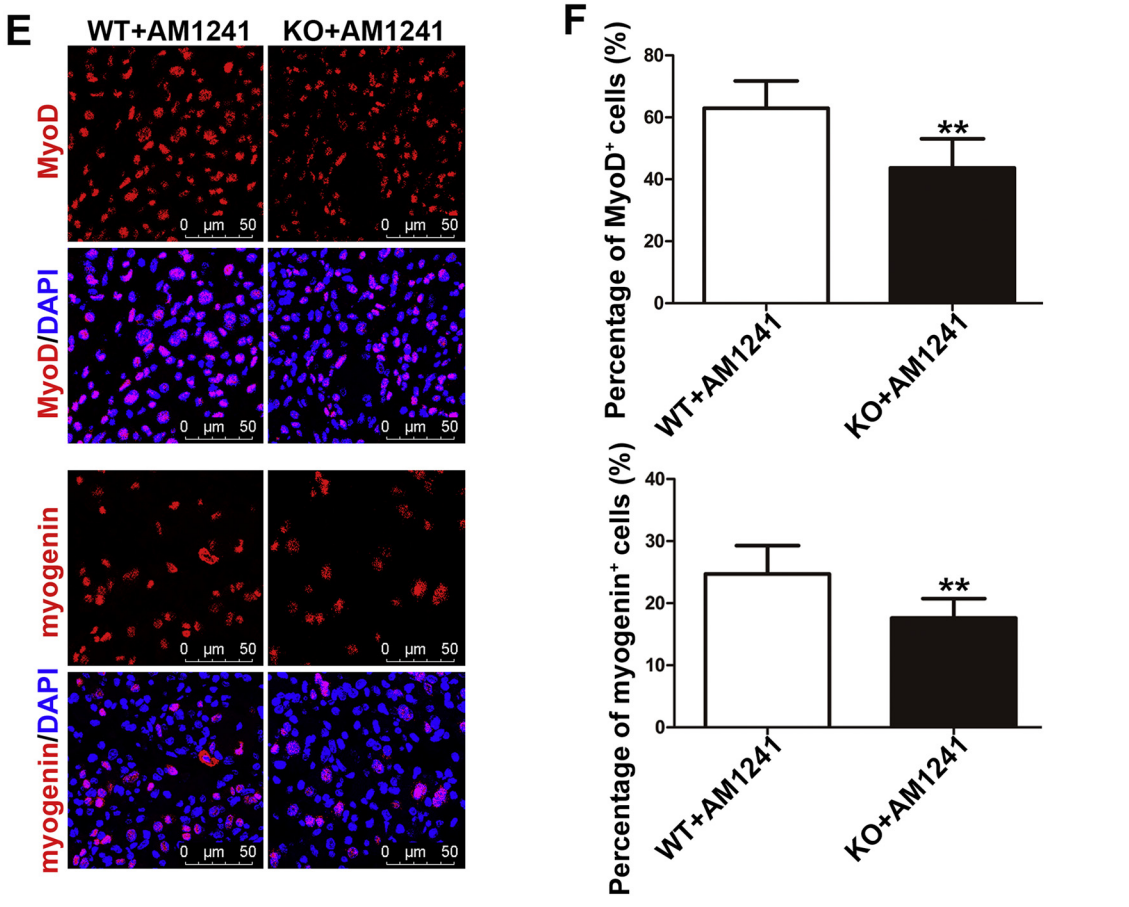

(caption on next page)

Fig. 4. Nrf2-deficient mice that were subjected to IRI exhibited deteriorative regeneration after CB_2 receptor activation. (A) Representative images of skeletal muscle 4 days after IRI showing H&E staining in the WT + AM1241 group (a) and *Nrf2* knockout + AM1241 group (b). Scale bar = 100 μm. (B) Quantification of the number of regenerating myotubes. (C) Protein expression of MyoD and myogenin 4 days after skeletal muscle IRI. (D) Quantification of MyoD and myogenin protein levels. (E) Immunofluorescent staining of MyoD and myogenin (red), with nuclei stained with DAPI (blue). Scale bar = 50 μm. (F) Nuclei were counted and depicted relative to the total number of skeletal muscle nuclei. The data are expressed as mean ± SD. $^{*}p < 0.05$, $^{**}p < 0.01$, compared with WT + AM1241 group ($n = 6$). (For interpretation of the references to colour in this figure legend, the reader is referred to the web version of this article.)

respectively) 4 days after IRI.

3.3. The antioxidative effect of CB_2 receptor activation was diminished by *Nrf2* deletion in IR-induced muscle lesions

Nrf2 is a master antioxidant transcription regulator. We evaluated the regulatory antioxidant effect of CB_2 receptor activation on Nrf2 expression by Western blot. As shown in Fig. 3A and B, IRI increased Nrf2 expression compared with the sham group. AM1241 treatment significantly increased Nrf2 expression compared with the vehicle group. The expression of HO-1, which is downstream of Nrf2, also similarly increased (Fig. 3A, B). We then subjected *Nrf2* knockout mice to IRI to further investigate whether the protective role of CB_2 receptor activation occurs through Nrf2 signaling. *Nrf2* knockout mice were treated with AM1241 after IRI, which resulted in a significant increase in muscle fiber injury, with more sarcoplasm dissolution and neutrophil infiltration (Fig. 3C) and a significant increase in histological damage scores compared with wildtype mice (Fig. 3D). The skeletal muscle W/D ratio in *Nrf2* knockout mice significantly increased compared with wildtype mice (Fig. 3E). Malondialdehyde levels significantly increased and SOD activity significantly decreased in *Nrf2* knockout mice compared with wildtype mice (Fig. 3F, G).

3.4. CB_2 receptor activation promoted early myogenesis, which was mitigated by *Nrf2* deletion in IR-induced muscle lesions

Next, we evaluated the role of Nrf2 in promoting myogenesis in *Nrf2* knockout and wildtype mice that were treated with AM1241. Nrf2 was immunostained in regenerating myotubes (Supplementary Fig. S1E). AM1241 treatment 4 days post-injury significantly decreased the number of regenerating myotubes in *Nrf2* knockout mice compared with wildtype mice (Fig. 4A, B and Supplementary Fig. S2A, B). MyoD and myogenin protein expression significantly decreased in *Nrf2* knockout mice compared with wildtype mice after treatment with AM1241 (Fig. 4C, D). Immunofluorescent staining showed that AM1241-induced CB_2 receptor activation 4 days post-injury significantly decreased MyoD- and myogenin-positive nuclei in *Nrf2* knockout mice compared with wildtype mice (43.72% ± 8.69% *vs.* 62.98% ± 8.12% and 17.61% ± 2.95% *vs.* 24.71% ± 4.29%; Fig. 4E, F).

3.5. CB_2 receptor activation attenuated H_2O_2-induced growth inhibition, ROS generation, and apoptosis, and these effects were diminished by of *Nrf2* knockdown in C2C12 myoblasts

We developed an *in vitro* model of oxidative damage in skeletal muscle. C2C12 myoblasts were exposed to 1 mM H_2O_2 similarly to a previous study [28]. AM1241 treatment at concentrations up to 10 μM did not cause any cytotoxic effects, whereas cell viability decreased at AM1241 concentrations of 20 and 30 μM (Supplementary Fig. S1F). C2C12 myoblasts were treated with 1, 2, 5, and 10 μM AM1241 12 h before 6 h H_2O_2 treatment, and cell viability was measured. The results showed that 1 mM H_2O_2 reduced cell viability by approximately 50%, which was consistent with a previous study [28]. Pretreatment with AM1241 significantly and dose-dependently prevented the H_2O_2-induced reduction of cell viability (Fig. 5A). Reactive oxygen species levels significantly and dose-dependently decreased in the presence of AM1241 (Fig. 5B, C). To further evaluate the cytoprotective effects of AM1241 on H_2O_2-induced apoptosis, the frequency of apoptotic myoblasts was detected by flow cytometry. Pretreatment with AM1241 before H_2O_2 exposure significantly and dose-dependently protected myoblasts against apoptosis (Fig. 5D). Western blot revealed a significant increase in the protein levels of cleaved caspase 3, a marker of apoptosis, in H_2O_2-treated myoblasts compared with control myoblasts, and pretreatment with AM1241 significantly decreased cleaved caspase 3 protein levels (Fig. 5E). Immunofluorescent staining showed that Nrf2 in control myoblasts was mainly localized in the cytoplasm but translocated to nuclei after AM1241 treatment (Fig. 5F). Western blot showed that non-cytotoxic concentrations of AM1241 dose-dependently increased Nrf2 and HO-1 protein expression and accumulation of Nrf2 in the nuclear fraction (Fig. 5G). To further evaluate the role of Nrf2 in H_2O_2-induced oxidative stress after AM1241 treatment, *Nrf2* knockdown myoblasts were used. The mRNA expression of Nrf2 significantly decreased in *Nrf2* knockdown myoblasts (Fig. 5H). After AM1241 treatment, H_2O_2-treated *Nrf2* knockdown myoblasts exhibited a decrease in cell viability compared with H_2O_2-treated Scr myoblasts (Fig. 5I). The protein levels of cleaved caspase 3 significantly increased in H_2O_2-treated *Nrf2* knockdown myoblasts compared with H_2O_2-treated Scr myoblasts (Fig. 5J).

3.6. CB_2 receptor activation promoted C2C12 myoblasts differentiation, and this effect was attenuated by *Nrf2* knockdown

To investigate the role of CB_2 receptor activation in muscle differentiation, we first examined differentiation-related morphology and the fusion index in C2C12 myoblasts. The replacement of proliferation medium (PM) with differentiation medium (DM) resulted in the time-dependent formation of multinucleated myotubes (Fig. 6A, B). To determine whether CB_2 receptor expression is induced during muscle differentiation, CB_2 receptor protein expression level was detected under PM and DM growth conditions. As shown in Fig. 6C, the expression of both CB_2 receptor and Nrf2 time-dependently increased in differentiated myotubes compared with proliferating myoblasts in PM. The levels of myosin heavy chain (MHC) and myogenin (*i.e.*, markers of muscle differentiation) also increased during cell differentiation. The mRNA expression of the CB_2 receptor, Nrf2, MHC, and myogenin significantly increased in differentiated myotubes compared with myoblasts in PM (Fig. 6D). Next, we examined whether CB_2 receptor activation affects myogenic differentiation. Treatment with AM1241 enhanced multinucleated myotubes formation and increased the fusion index (Fig. 6E, F), with increases in the protein levels of MHC, myogenin, and Nrf2 compared with the vehicle group (Fig. 6G). To further investigate the involvement of Nrf2 in the ability of CB_2 receptor activation to promote C2C12 myoblasts differentiation, cell differentiation was induced in *Nrf2* knockdown C2C12 myoblasts. After AM1241 treatment, Nrf2 knockdown suppressed myotubes formation and decreased the fusion index (Fig. 6H, I), with decreases in the expression of Nrf2, myogenin, and MHC compared with Scr myoblasts (Fig. 6J).

4. Discussion

Skeletal muscle IRI is a common and serious pathological process in clinical medicine. The sequelae of cellular IRI can lead to the loss of limb function, or even death [1]. The role of CB_2 receptor in skeletal muscle IRI is unclear. Our previous studies showed that CB_2 receptor activation has a beneficial effect on rat skeletal muscle contusion by

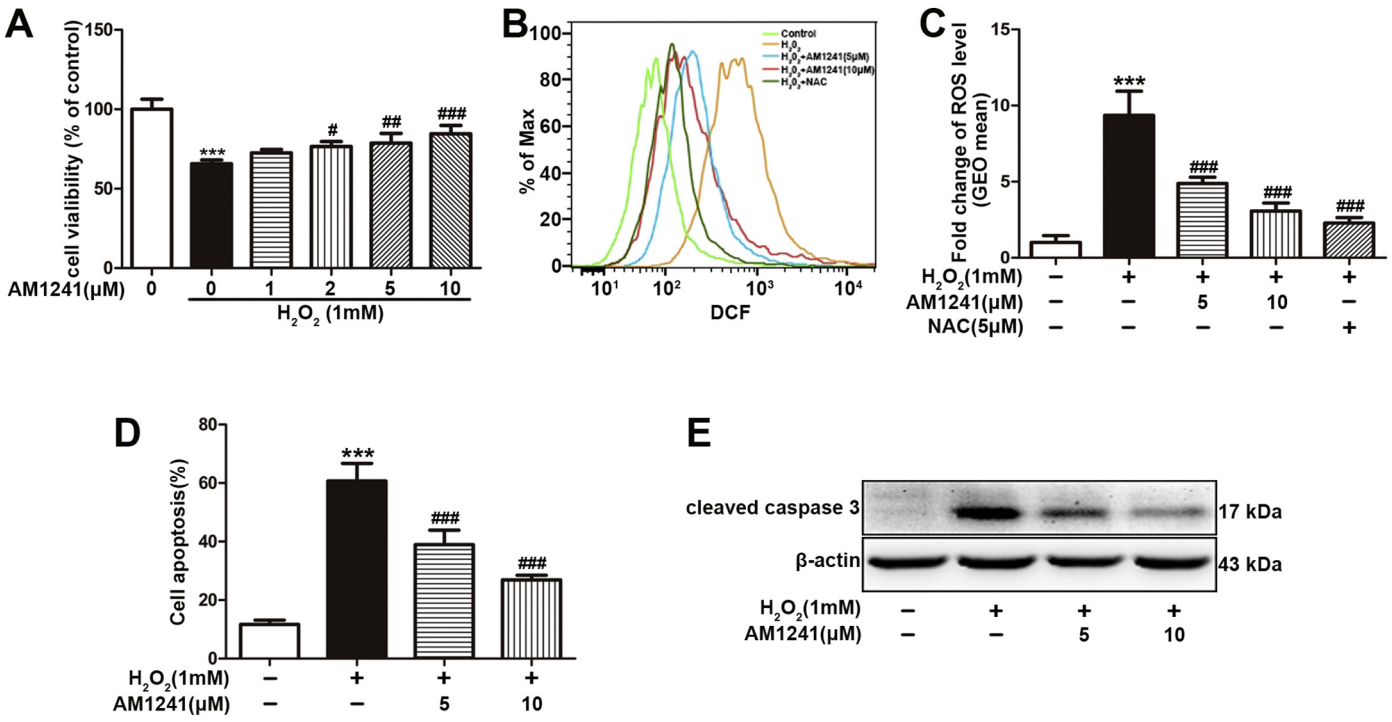

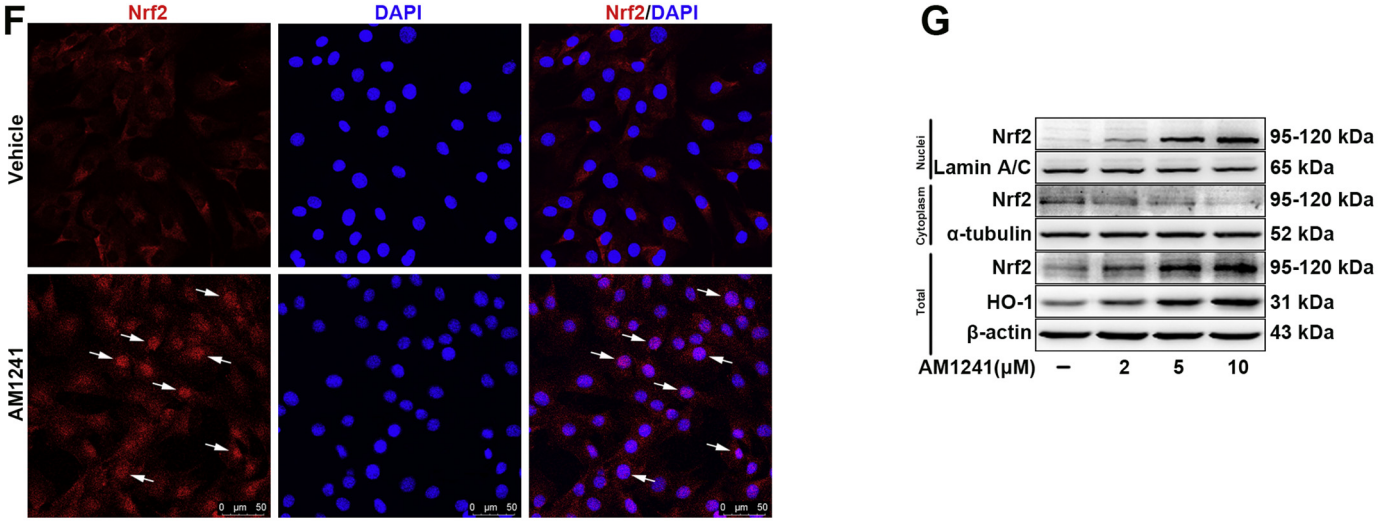

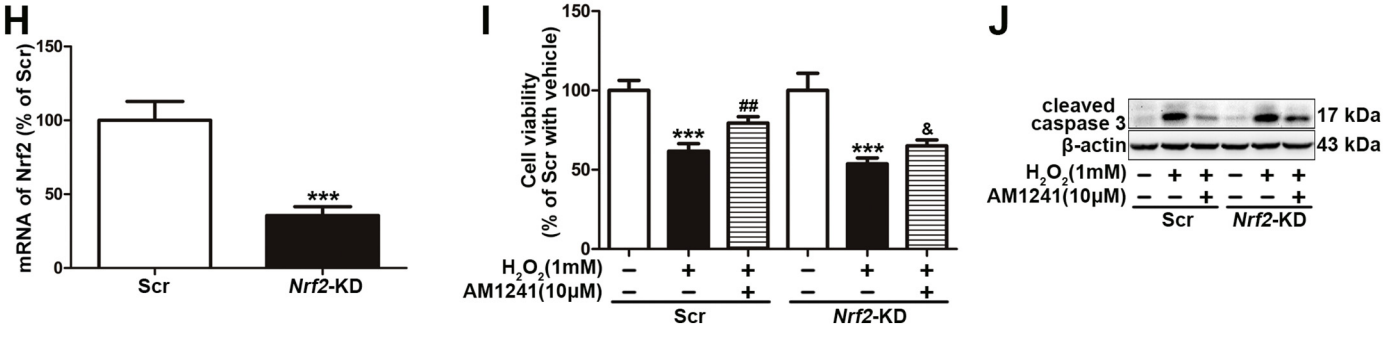

(caption on next page)

Fig. 5. CB_2 receptor activation protects C2C12 myoblasts against H_2O_2-induced damage *via* Nrf2 signaling. (A) C2C12 myoblasts were pretreated with or without AM1241 at the indicated concentrations for 12 h before exposure to 1 mM H_2O_2 for an additional 6 h. Cell viability was measured by the MTT assay. The data are expressed as mean ± SD. $^{***}p < 0.001$, compared with control group; $^{\#}p < 0.05$, $^{\#\#}p < 0.05$, $^{\#\#\#}p < 0.001$, compared with H_2O_2 group ($n = 6$). (B) Flow cytometry analysis of ROS production in C2C12 myoblasts after the indicated treatment. (C) Quantification of ROS production. (D) Quantification of C2C12 myoblasts apoptosis by flow cytometry after the indicated treatment. (E) Levels of cleaved caspase 3, determined by Western blot after the indicated treatment. The data are expressed as mean ± SD. $^{***}p < 0.001$, compared with control group; $^{\#}p < 0.05$, $^{\#\#}p < 0.01$, $^{\#\#\#}p < 0.001$, compared with H_2O_2 group ($n = 6$). (F) Representative images of immunofluorescent staining of Nrf2 in C2C12 myoblasts. C2C12 myoblasts were treated with AM1241 (lower panel) or vehicle (upper panel) for 6 h. Red fluorescence indicates Nrf2-positive cells. Blue fluorescence indicates DAPI. The arrows indicate the nuclear translocation of Nrf2. Scale bar = 50 μm. (G) Levels of Nrf2 and HO-1 were determined by Western blot after the indicated treatment. (H) The mRNA expression of Nrf2 was determined by real-time reverse-transcription quantitative PCR in Scr and *Nrf2* knockdown myoblasts. $^{***}p < 0.001$, compared with Scr myoblasts ($n = 6$). (I) Scrambled or *Nrf2* knockdown C2C12 myoblasts were pretreated with 10 μM AM1241 or vehicle for 12 h before exposure to 1 mM H_2O_2 for an additional 6 h. Cell viability was measured by the MTT assay. The data are expressed as mean ± SD. $^{***}p < 0.001$, compared with vehicle group in the same myoblasts; $^{\#\#}p < 0.01$, compared with H_2O_2 group in the same myoblasts; $^{\&}p < 0.05$, compared with Scr myoblasts with the same treatment ($n = 6$). (J) Levels of cleaved caspase 3, determined by Western blot after the indicated treatment. (For interpretation of the references to colour in this figure legend, the reader is referred to the web version of this article.)

inhibiting inflammation and fibrosis [14,15]. We speculated that CB_2 receptor activation might be involved in the modulation of skeletal muscle IRI and play a beneficial role in this pathological condition. In the present study, intensive immunoreactivity of CB_2 receptor was detected in regenerated myotubes following skeletal muscle IRI, and CB_2 receptor activation exerted protective effects against skeletal muscle IRI by alleviating skeletal muscle oxidative damage and accelerating early myogenesis. CB_2 receptor activation also protected C2C12 myoblasts from H_2O_2-induced oxidative injury and promoted C2C12 myoblasts differentiation *in vitro*. Nrf2 deletion impaired these aforementioned beneficial effects of CB_2 receptor activation both *in vivo* and *in vitro*. Altogether, our findings elucidate the beneficial roles of CB_2 receptor and Nrf2 in skeletal muscle IRI, suggesting a possible treatment for IR-induced skeletal muscle injury.

Previous studies have sought to develop interventions that ameliorate muscle damage to improve the prognosis of skeletal muscle IRI and minimize patient morbidity and mortality [1]. Our results demonstrate that CB_2 receptor activation *in vivo* limits IR-induced histopathological lesions, edema, and neutrophil infiltration. These results are consistent with previous studies that reported a beneficial effect of CB_2 receptor activation against IRI in other organs [13,29,30]. Reactive oxygen species have been considered to be the main factors that are responsible for local and systemic damage that is caused by IRI [1,31]. The generation of ROS initiates lipid peroxidation and inactivates antioxidative stress-related proteins [32], leading to the continuous necrosis of skeletal muscle myocytes and apoptosis and aggravating IRI [4]. The elimination of ROS has been shown to attenuate skeletal muscle IRI under various conditions [31]. We found that CB_2 receptor activation is associated with a reduction of oxidative stress in skeletal muscle IRI *in vivo*, reflected by a decrease in MDA levels and increase in SOD activity. These data were reinforced by our *in vitro* experiments in C2C12 myoblasts, in which we found a direct protective effect of CB_2 receptor activation on skeletal muscle myocyte survival under conditions of H_2O_2-induced oxidative stress. These results emphasize the protective role of CB_2 receptor activation that is attributable to its effect against oxidative stress [33] in cases of limb injury that is caused by IR.

Cannabinoid signaling regulates cell survival and modulates progenitor/stem cell proliferation and differentiation, with different outcomes that depend on specific molecular targets and the cellular context [34]. Muscle regeneration is a critical event for the functional recovery of injured skeletal muscle. Upon muscle injury, SCs are first activated and then begin to proliferate, differentiate, and fuse, leading to new myofiber formation and the reconstitution of a functional contractile apparatus [35,36]. The microenvironment of SCs regulates their function by inducing myogenic regulatory factors, such as MyoD and Myogenin [5,36,37]. In the present study, regenerating myotubes expressed CB_2 receptor, and CB_2 receptor protein level significantly increased during C2C12 myoblasts differentiation, thus supporting the possibility that CB_2 receptor plays a role in the muscle regeneration process. Myotubes significantly regenerated, reflected by upregulation of the expression of MyoD and myogenin after CB_2 receptor activation. These findings were confirmed by our *in vitro* observations, in which multinucleated myotubes formation increased, reflected by increases in the protein levels of markers of muscle differentiation, indicating the enhancement of muscle regeneration capacity. Previous studies showed that CB_2 receptor activation promoted the regeneration of dopamine neurons in Parkinson's disease mice [38] and liver regeneration following acute liver insult [39]. The activation of CB_2 receptor enhances the osteogenic differentiation of bone marrow-derived mesenchymal stem cells [40] and accelerates the onset of spermatogenesis [41]. Interestingly, skeletal muscle regeneration and muscle differentiation are tightly controlled by redox balance [6,42]. The acceleration of muscle regeneration in IRI is likely attributable to proliferation and differentiation that either are directly modulated by CB_2 receptor [34] or indirectly occur through the effects of CB_2 receptor activation on oxidative stress [19,33].

Nrf2 is a key regulator that protects against oxidative stress injury [17]. Multiple studies have provided evidence that the disruption of Nrf2 leads to higher ROS levels, functional deficits, histopathological alterations [43], and increases in apoptotic cells after skeletal muscle IRI [44] and in aging skeletal muscle myocytes [9]. In the present study, CB_2 receptor activation exerted muscle-protective effects by improving the nuclear translocation of Nrf2 and upregulating HO-1. The genetic silencing of Nrf2 attenuated the protective effect of CB_2 receptor activation on IR-induced oxidative damage and H_2O_2-induced C2C12 myoblasts damage. These results suggest that the protective role of CB_2 receptor activation in skeletal muscle IRI might be associated with the Nrf2-regulated antioxidant response. These findings are consistent with previous studies that found that CB_2 receptor activation enhanced Nrf2 activation, improving cardiac function and repair in mice that were subjected to myocardial infarction [20,21] and reducing neurotoxicity that was induced by lipopolysaccharide [22] and glutamate [23] *in vitro*. Overall, CB_2 receptor activation appears to ameliorate IR-induced oxidative damage partially through Nrf2 signaling.

The contribution of Nrf2 to protect against exogenous and endogenous oxidative stress has been well established. Emerging evidence indicates that Nrf2 also has various novel functions, especially with regard to cell proliferation and differentiation [19]. Nrf2 augments skeletal muscle regeneration after IRI by directly enhancing MyoD expression [5]. Nrf2 knockout mice exhibited slower regeneration, reflected by impairments in the activation of stem cells after cardiotoxin (CTX) injury [8]. *In vitro* studies have shown that activated Nrf2 serves as a transcription factor during muscle differentiation [42,45], and Nrf2 deficiency impairs muscle differentiation [42]. In the present study, Nrf2 deficiency attenuated the role of CB_2 receptor in promoting early myogenesis in mice that were subjected to IRI, and this finding was confirmed by our *in vitro* experiments in C2C12 myoblasts. The acceleration of cell differentiation that was induced by CB_2 receptor activation was blocked by Nrf2 knockdown. These observations indicate that CB_2 receptor activation enhances skeletal muscle regeneration partly through Nrf2 signaling.

In conclusion, the present study revealed a highly beneficial effect

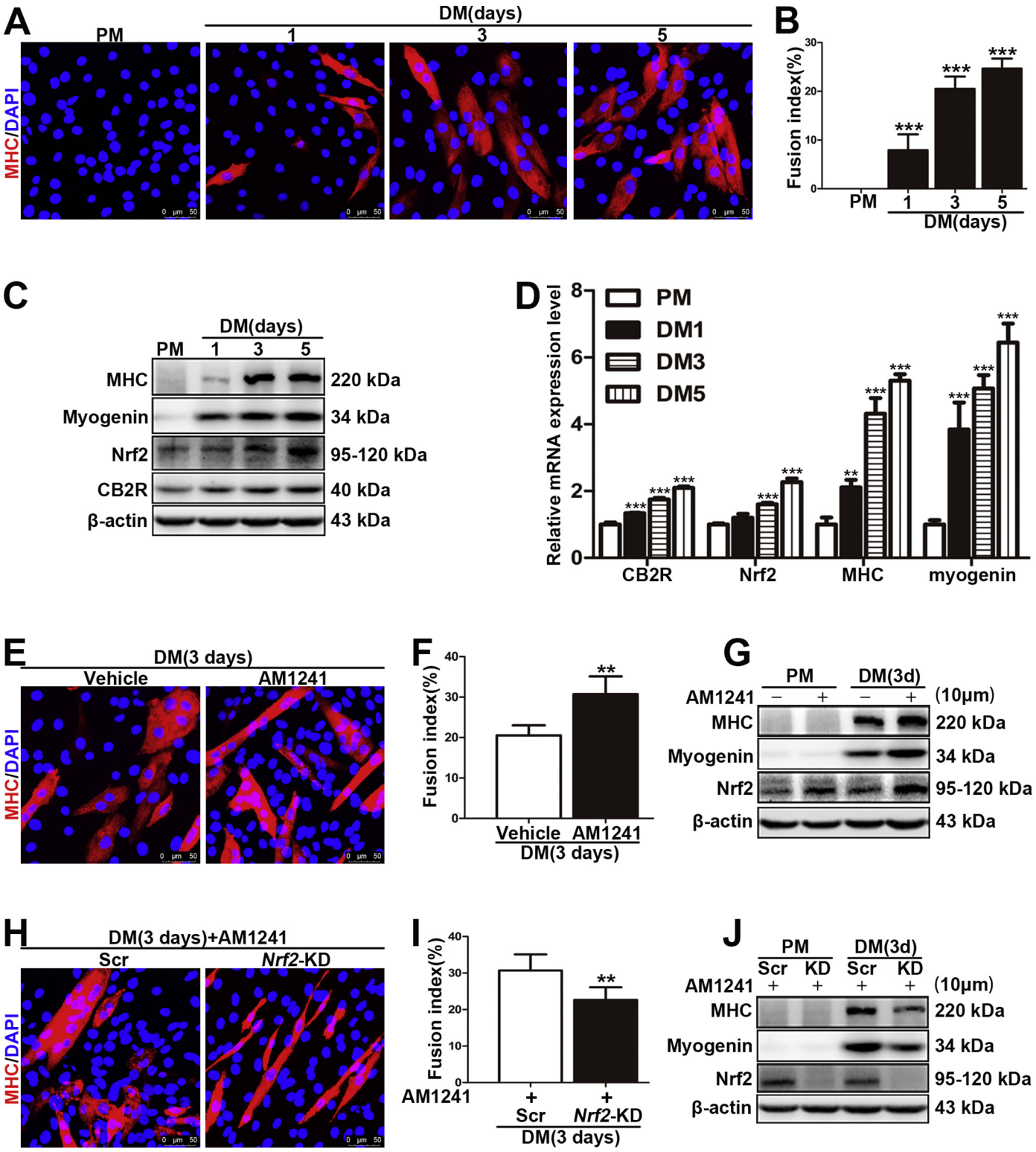

Fig. 6. CB_2 receptor activation enhances C2C12 myoblasts differentiation *via* Nrf2 signaling. (A–D) C2C12 myoblasts were incubated in DM for 1, 3, and 5 days. (A) Representative images of MHC (red) immunofluorescence staining at different differentiation intervals. Scale bars = 50 μm. (B) Fusion index. (C) Levels of CB_2 receptor, Nrf2, MHC, and myogenin, determined by Western blot. (D) mRNA expression of CB_2 receptor, Nrf2, MHC, and myogenin. The data are expressed as mean ± SD. $^{**}p < 0.01$, $^{***}p < 0.001$, compared with myoblasts cultured in PM ($n = 6$). (E–G) C2C12 myoblasts were incubated in DM with AM1241 or vehicle for 3 days. (E) Representative images of MHC (red) immunofluorescence staining in the different groups. Scale bars = 50 μm. (F) Fusion index. (G) Levels of Nrf2 and myocyte differentiation markers were determined by Western blot. The data are expressed as mean ± SD. $^{**}p < 0.01$, compared with vehicle group ($n = 6$). (H–J) *Nrf2* knockdown or Scr myoblasts were incubated in DM with AM1241 for 3 days. (H) Representative images of MHC (red) immunofluorescence staining in the different groups. Scale bars = 50 μm. (I) Fusion index. (J) Levels of Nrf2 and myocyte differentiation markers, determined by Western blot. The data are expressed as mean ± SD. $^{**}p < 0.01$, compared with Scr myoblasts grown in DM with AM1241 ($n = 6$). (For interpretation of the references to colour in this figure legend, the reader is referred to the web version of this article.)

of CB_2 receptor activation on post-IR oxidative damage and early myogenesis in skeletal muscle that occurred partly *via* Nrf2 signaling. Our results provide novel evidence of the pivotal roles of CB_2 receptor activation and Nrf2 expression in regulating repair after skeletal muscle injury. These findings may contribute to the discovery of new therapeutic targets to protect skeletal muscle from IRI or trauma.

5. Limitations

Despite the clinical relevance of the present findings, our study has some limitations. Firstly, to preclude the effects of endocrine system difference and ensure the uniformity of the experimental results, only male mice were recruited in our study, female biology by including female animals should be considered in future work. Secondly, *In vitro* studies, it's better to use SCs isolated from intact skeletal muscle, which might more characterize skeletal muscle regeneration, although C2C12 myoblasts cell line proliferated from SCs. Thirdly, previous studies have shown that many compounds activate the transcription of various antioxidant genes through a PI3K/Akt/Nrf2 mechanism [46,47], and CB_2 receptor regulate PI3K/Akt pathway in most cell systems [34]. CB_2 receptor activation may improve cardiac function through PI3K/Akt/Nrf2 signaling [20]. However, in skeletal muscle IRI, the pathway connecting CB_2 receptor with Nrf2 needs to be clarified.

Supplementary data to this article can be found online at https://doi.org/10.1016/j.lfs.2019.05.056.

Author contributions

This experiment was carried out in collaboration between all authors. Dawei Guan, Rui Zhao and Jingbo Pi defined the research theme, and designed methods and experiments. Mengzhou Zhang, Penghao Jiang and Yingfu Sun carried out the laboratory experiments and interpreted the results, Mengzhou Zhang, Dawei Guan and Rui Zhao wrote the paper. Miao Zhang, Linlin Wang, Tianshui Yu and Shukun Jiang revised the paper. All authors had responsibility for the final content.

Declaration of Competing Interest

The authors have declared that no competing interest exists.

Acknowledgements

This research was financially supported by grants from the National Natural Science Foundation of China (No. 81671862, 81871529, 81801874, 81772023).

References

[1] S. Gillani, J. Cao, T. Suzuki, et al., The effect of ischemia reperfusion injury on skeletal muscle, Injury 43 (2012) 670–675, https://doi.org/10.1016/j.injury.2011.03.008.
[2] C. Gürsul, F.N. Ekinci Akdemir, T. Akkoyun, et al., Protective effect of Naringin on experimental hindlimb ischemia/reperfusion injury in rats, J. Enzyme Inhib. Med. Chem. 31 (2016) 56–61, https://doi.org/10.3109/147 56366.2016.1167050.
[3] T. Huang, W. Wang, C. Tu, et al., Hydrogen-rich saline attenuates ischemia–reperfusion injury in skeletal muscle, J. Surg. Res. 194 (2015) 471–480, https://doi.org/10.1016/j.jss.2014.12.016.
[4] W.Z. Wang, X.H. Fang, L.L. Stephenson, et al., Melatonin attenuates I/R-induced mitochondrial dysfunction in skeletal muscle, J. Surg. Res. 171 (2011) 108–113, https://doi.org/10.1016/j.jss.2010.01.019.
[5] O. Al-Sawaf, A. Fragoulis, C. Rosen, et al., Nrf2 augments skeletal muscle regeneration after ischaemia-reperfusion injury, J. Pathol. 234 (2014) 538–547, https://doi.org/10.1002/path.4418.
[6] E. Le Moal, V. Pialoux, G. Juban, et al., Redox control of skeletal muscle regeneration, Antioxid. Redox Signal. 27 (2017) 276–310, https://doi.org/10.1089/ars.2016.6782.
[7] C. Sciorati, E. Rigamonti, A.A. Manfredi, et al., Cell death, clearance and immunity in the skeletal muscle, Cell Death Differ. 23 (2016) 927–937, https://doi.org/10.1038/cdd.2015.171.
[8] S.B. Shelar, M. Narasimhan, G. Shanmugam, et al., Disruption of nuclear factor (erythroid-derived-2)-like 2 antioxidant signaling: a mechanism for impaired activation of stem cells and delayed regeneration of skeletal muscle, FASEB J. 30 (2016) 1865–1879, https://doi.org/10.1096/fj.201500153.
[9] M. Narasimhan, J. Hong, N. Atieno, et al., Nrf2 deficiency promotes apoptosis and impairs PAX7/MyoD expression in aging skeletal muscle cells, Free Radic. Biol. Med. 71 (2014) 402–414, https://doi.org/10.1016/j.fr eeradbiomed.2014.02.023.
[10] T.S. Yu, Z.H. Cheng, L.Q. Li, et al., The cannabinoid receptor type 2 is time-dependently expressed during skeletal muscle wound healing in rats, Int. J. Legal Med. 124 (2010) 397–404, https://doi.org/10.1007/s00414-010-0465-1.
[11] V. Di Marzo, M. Bifulco, L. De Petrocellis, The endocannabinoid system and its therapeutic exploitation, Nat. Rev. Drug Discov. 3 (2004) 771–784, https://doi.org/10.1038/nrd1495.
[12] L. Li, D. Yun, Y. Zhang, et al., A cannabinoid receptor 2 agonist reduces blood-brain barrier damage via induction of MKP-1 after intracerebral hemorrhage in rats, Brain Res. 1697 (2018) 113–123, https://doi.org/10.1016/j.brainres.2018.06.006.
[13] B. Horváth, L. Magid, P. Mukhopadhyay, et al., A new cannabinoid CB2 receptor agonist HU-910 attenuates oxidative stress, inflammation and cell death associated with hepatic ischaemia/reperfusion injury, Br. J. Pharmacol. 165 (2012) 2462–2478, https://doi.org/10.1111/j.1476-5381.2011.01381.x.
[14] T. Yu, X. Wang, R. Zhao, et al., Beneficial effects of cannabinoid receptor type 2 (CB2R) in injured skeletal muscle post-contusion, Histol. Histopathol. 30 (2015) 737–749, https://doi.org/10.14670/HH-30.737.
[15] M. Zhang, S.K. Jiang, Z.L. Tian, et al., CB2R orchestrates fibrogenesis through regulation of inflammatory response during the repair of skeletal muscle contusion, Int. J. Clin. Exp. Pathol. 8 (2015) 3491–3502 https://www ncbi.nlm.nih.gov/pmc/articles/PMC4466920.
[16] F.A. Iannotti, C. Silvestri, E. Mazzarella, et al., The endocannabinoid 2-AG controls skeletal muscle cell differentiation via CB1 receptor-dependent inhibition of Kv7 channels, Proc. Natl. Acad. Sci. U. S. A. 111 (2014) E2472–E2481, https://doi.org/10.1073/pnas.1406728111.
[17] A. Anedda, E. Lopez-Bernardo, B. Acosta-Iborra, et al., The transcription factor Nrf2 promotes survival by enhancing the expression of uncoupling protein 3 under conditions of oxidative stress, Free Radic. Biol. Med. 61 (2013) 395–407, https://doi.org/10.1016/j.freeradbiomed.2013.04.007.
[18] N. Wakabayashi, S.L. Slocum, J.J. Skoko, et al., When NRF2 talks, who's listening? Antioxid. Redox Signal. 13 (2010) 1649–1663, https://doi.org/10.1089/ars.2010.3216.
[19] S. Murakami, H. Motohashi, Roles of Nrf2 in cell proliferation and differentiation, Free Radic. Biol. Med. 88 (2015) 168–178, https://doi.org/10.1016/j.freeradbiomed.2015.06.030.
[20] Y. Wang, S. Ma, Q. Wang, et al., Effects of cannabinoid receptor type 2 on endogenous myocardial regeneration by activating cardiac progenitor cells in mouse infarcted heart, Sci. China Life Sci. 57 (2014) 201–208, https://doi.org/10.1007/s11427-013-4604-z.
[21] X. Li, D. Han, Z. Tian, et al., Activation of cannabinoid receptor type II by AM1241 ameliorates myocardial fibrosis via Nrf2-mediated inhibition of TGF-β1/Smad3 pathway in myocardial infarction mice, Cell. Physiol. Biochem. 39 (2016) 1521–1536, https://doi.org/10.1159/000447855.
[22] V.R. Askari, R. Shafiee-Nick, Promising neuroprotective effects of beta-caryophyllene against LPS-induced oligodendrocyte toxicity: a mechanistic study, Biochem. Pharmacol. 159 (2018) 154–171, https://doi.org/10.1016/j.bcp.2018.12.001.
[23] L.C. Assis, M.R. Straliotto, D. Engel, et al., Beta-caryophyllene protects the C6 glioma cells against glutamate-induced excitotoxicity through the Nrf2 pathway, Neuroscience 279 (2014) 220–231, https://doi.org/10.1016/j. neuroscience.2014.08.043.
[24] W. Dong, B. Yang, L. Wang, et al., Curcumin plays neuroprotective roles against traumatic brain injury partly via Nrf2 signaling, Toxicol. Appl. Pharmacol. 346 (2018) 28–36, https://doi.org/10.1016/j.taap.2018.03.020.
[25] R.S. Crawford, F.F. Hashmi, J.E. Jones, et al., A novel model of acute murine hindlimb ischemia, Am. J. Physiol. Heart Circ. Physiol. 292 (2007) H830–H837, https://doi.org/10.1152/ajpheart.00581.2006.
[26] H. Zong, X. Li, H. Lin, et al., Lipoxin A4 pretreatment mitigates skeletal muscle ischemia-reperfusion injury in rats, Am. J. Transl. Res. 9 (2017) 1139–1150 https://www.ncbi.nlm.nih.gov/pmc/articles/PMC5376005/.
[27] J. Pi, L. Leung, P. Xue, et al., Deficiency in the nuclear factor E2-related factor-2 transcription factor results in impaired adipogenesis and protects against diet-induced obesity, J. Biol. Chem. 285 (2010) 9292–9300, https://doi.org/10.1074/jbc.M109.093955.
[28] J. Kang, M. Han, G. Kim, et al., Nrf2-mediated HO-1 induction contributes to antioxidant capacity of a Schisandrae Fructus ethanol extract in C2C12 myoblasts, Nutrients 6 (2014) 5667–5678, https://doi.org/10.3390/nu6125667.
[29] Q. Li, F. Wang, Y. Zhang, et al., Activation of cannabinoid type 2 receptor by JWH133 protects heart against ischemia/reperfusion-induced apoptosis, Cell. Physiol. Biochem. 31 (2013) 693–702, https://doi.org/10.1159/ 000350088.
[30] F. Montecucco, S. Lenglet, V. Braunersreuther, et al., CB2 cannabinoid receptor activation is cardioprotective in a mouse model of ischemia/reperfusion, J. Mol. Cell. Cardiol. 46 (2009) 612–620, https://doi.org/10.1016/j.yj mcc.2008.12.014.
[31] W.Z. Wang, R.C. Baynosa, W.A. Zamboni, Therapeutic interventions against reperfusion injury in skeletal muscle, J. Surg. Res. 171 (2011) 175–182, https://doi.org/10.1016/j.jss.2011.07.015.
[32] J.M. Lee, J. Li, D.A. Johnson, et al., Nrf2, a multi-organ protector? FASEB J. 19 (2005) 1061–1066, https://doi.org/10.1096/fj.04-2591hyp.
[33] P. Pacher, G. Hasko, Endocannabinoids and cannabinoid receptors in ischaemia-reperfusion injury and preconditioning, Br. J. Pharmacol. 153 (2008) 252–262, https://doi.org/10.1038/sj.bjp.0707582.

[34] I. Galve-Roperh, V. Chiurchiu, J. Diaz-Alonso, et al., Cannabinoid receptor signaling in progenitor/stem cell proliferation and differentiation, Prog. Lipid Res. 52 (2013) 633–650, https://doi.org/10.1016/j.plipres.2013.0 5.004.
[35] T.A. Jarvinen, T.L. Jarvinen, M. Kaariainen, et al., Muscle injuries: biology and treatment, Am. J. Sports Med. 33 (2005) 745–764, https://doi.org/10.1177/0363546505274714.
[36] S.B. Charge, M.A. Rudnicki, Cellular and molecular regulation of muscle regeneration, Physiol. Rev. 84 (2004) 209–238, https://doi.org/10.1152/physrev.00019.2003.
[37] M.A. Rudnicki, F. Le Grand, I. McKinnell, et al., The molecular regulation of muscle stem cell function, Cold Spring Harb. Symp. Quant. Biol. 73 (2008) 323–331, https://doi.org/10.1101/sqb.2008.73.064.
[38] J. Shi, Q. Cai, J. Zhang, et al., AM1241 alleviates MPTP-induced Parkinson's disease and promotes the regeneration of DA neurons in PD mice, Oncotarget 8 (2017) 67837–67850, https://doi.org/10.18632/oncotarge t.18871.
[39] F. Teixeira-Clerc, M.P. Belot, S. Manin, et al., Beneficial paracrine effects of cannabinoid receptor 2 on liver injury and regeneration, Hepatology 52 (2010) 1046–1059, https://doi.org/10.1002/hep.23779.
[40] Y.X. Sun, A.H. Xu, Y. Yang, et al., Activation of cannabinoid receptor 2 enhances osteogenic differentiation of bone marrow derived mesenchymal stem cells, Biomed. Res. Int. 2015 (2015) 874982, , https://doi.org/10.1155/ 2015/874982.
[41] D. Di Giacomo, E. De Domenico, C. Sette, et al., Type 2 cannabinoid receptor contributes to the physiological regulation of spermatogenesis, FASEB J. 30 (2016) 1453–1463, https://doi.org/10.1096/fj.15-279034.
[42] S. Lim, J.Y. Shin, A. Jo, et al., Carbonyl reductase 1 is an essential regulator of skeletal muscle differentiation and regeneration, Int. J. Biochem. Cell Biol. 45 (2013) 1784–1793, https://doi.org/10.1016/j.biocel.2013.05.025.
[43] P. Kombairaju, J.P. Kerr, J.A. Roche, et al., Genetic silencing of Nrf2 enhances X-ROS in dysferlin-deficient muscle, Front. Physiol. 5 (2014) 57, https://doi.org/10.3389/fphys.2014.00057.
[44] O. Al-Sawaf, A. Fragoulis, C. Rosen, et al., Nrf2 protects against TWEAK-mediated skeletal muscle wasting, Sci. Rep. 4 (2014) 3625, , https://doi.org/10.1038/srep03625.
[45] Y. Ding, K.J. Choi, J.H. Kim, et al., Endogenous hydrogen peroxide regulates glutathione redox via nuclear factor erythroid 2-related factor 2 downstream of phosphatidylinositol 3-kinase during muscle differentiation, Am. J. Pathol. 172 (2008) 1529–1541, https://doi.org/10.2353/ajpath.2008.070429.
[46] G. Yu, Y. Guan, L. Liu, et al., The protective effect of low-energy shock wave on testicular ischemia-reperfusion injury is mediated by the PI3K/AKT/NRF2 pathway, Life Sci. 213 (2018) 142–148, https://doi.org/10.1016/j.lfs. 2018.10.021.
[47] Q. Ma, Transcriptional responses to oxidative stress: pathological and toxicological implications, Pharmacol. Ther. 125 (2010) 376–393, https://doi.org/10.1016/j.pharmthera.2009.11.004.